Preparation, spectroscopic and structural study of copper(II) complexes derived from bulky pyridine ligands

Miguel Guerrero [a,b], José A. Ayllón [a,*], Teresa Calvet [c], Mercè Font-Bardia [d], Josefina Pons [a,*]

a Departament de Química, Universitat Autònoma de Barcelona, 08193-Bellaterra, Barcelona, Spain

b Departament de Física, Universitat Autònoma de Barcelona, 08193-Bellaterra, Barcelona, Spain

c Cristal·lografia, Mineralogia i Dipòsits Minerals, Universitat de Barcelona, Martí i Franquès s/n, 08028 Barcelona, Spain

d Unitat de Difracció de Raig-X, Centres Científics i Tecnològics de la Universitat de Barcelona (CCiTUB), Universitat de Barcelona, Solé i Sabarís, 1-3, 08028 Barcelona, Spain

.

ABSTRACT:

Three different binuclear tetracarboxylato-bridged copper(II) complexes supported by bulky pyridines ligands [Cu(m-MeCO2)2(dPy)]2 (dPy = 3-phenylpyridine (1), 2-benzylpyridine (2) and 4-acetylpyridine (3)) have been synthesised. These compounds were obtained from reaction of [Cu(MeCO2)2(H2O)]2 with pyridine-derived ligands in methanol at room temperature. All compounds were fully characterized by analytical and spectroscopic methods. The molecular structures were determined by X-ray diffraction analysis. All compounds consist of binuclear units where both Cu(II) atoms are linked by four syn–syn carboxylates bridges, showing a paddle-wheel unit, and exhibit interesting intermolecular interactions in the outer coordination sphere.

1. INTRODUCTION

Self-assembly of copper(II) cations through a mixed ligand strategy has progressively become an innovative approach, which generates frameworks with more diverse structures and, therefore, new and unexpected properties [1]. Copper(II) shows different coordination numbers and geometries. Thus, their complexes and solid-state compounds possess an array of different redox, magnetic, optical and electrical properties because of their fascinating topologies and intriguing frameworks [2].

The synthesis, crystal structure and properties of several copper (II) carboxylates have already been extensively studied, in particular with pyridine groups have garnered great interest due to their diverse structural features [3], spectroscopic, magnetic and catalytic activities [4]. Furthermore, a large number of paddle-wheel type binuclear copper(II) carboxylate adducts [Cu(RCO2)2(L)]2, where L is an apical ligand with oxygen or nitrogen atom, have been reported in the literature [5]. In their synthesis metal carboxylates, along with NA and OA donor atoms, have often been used with the aim of constructing paddle-wheel with mixed ligands, which might have interesting structural features with useful applications.

As a continuing effort to enhance the structure, reactivity and different properties of the copper(II) compounds, we employed pyridylamines ligands with the potential to incorporate intraand intermolecular interactions (e.g. hydrogen bond, p–p stacking, etc) [1a,b]. In this context, we have studied the synthesis and structural characterization of 1,3-benzodioxole-5-carboxylic acid (HPip) and different amines (3-phenylpyridine and 4-phenylpyridine) with Zn(MeCO2)2 2H2O and Cd(MeCO2)2 2H2O obtaining the compounds [Zn(m-Pip)2(3-Phpy)]2, [Zn(m-Pip)2(4-Phpy)]2, [Cd(m-Pip) (Pip)(3-Phpy)2]2 and [Cd(m-Pip)(Pip)(4-Phpy)2]2 coordination dimers [6]. Also studied the reaction of the same ligand (HPip) with [Cu(MeCO2)2(H2O)]2 and pyridine ligands (dPy = 3-Phpy, 4-Bzpy and 4-Phpy) obtaining [Cu(Pip)2(3-Phpy)(H2O)] and [Cu(Pip)2-(4-Bzpy)2][Cu(Pip)2(4-Bzpy)2(HPip)] monomeric and [Cu(m-Pip)2-(dPy]2 (dPy = 3-Phpy, 4-Bzpy) and [Cu(m-Pip)(Pip)(4-Phpy)2]2 dimeric compounds [7]. Moreover, when the reaction of HPip and [Cu(MeCO2)2(H2O)]2 in 1:1 M:L is assayed, another compound is obtained [Cu(m-Pip)(m-MeCO2)(MeOH)]2 [8].

In this manuscript, we are interested in the reaction of [Cu(MeCO2)2(H2O)]2 compound with bulky amine derivatives, with the finality of replacing H2O for different amines, and studied novel supramolecular systems with the potential applications in gas storage/separation and catalysis. In particular, we show the synthesis, IR spectroscopy and X-ray crystal structure of three paddle- wheel copper complexes, [Cu(m-MeCO2)2(dPy)]2 (dPy = 3-phenylpyridine (1), 2-benzylpyridine (2) and 4-acetylpyridine (3)), which are obtained from copper(II) acetate and different pyridylamines.

.

2. RESULTS AND DISCUSSION

2.1. Synthesis and general characterization

Complexes 1–3, were prepared in MeOH at room temperature via combination of the [Cu(m-MeCO2)2(H2O)]2 salt, 3-phenylpyridine (3-Phpy) (1), 2-benzylpyridine (2-Bzpy) (2), and 4-acetylpyridine (4-Acpy) (3) with ratio 1:1. In these reactions, H2O solvent were displaced by bulky amine ligands. The corresponding crystals suitable for X-ray crystallographic analysis were grown via slow evaporation of their solution. The three compounds were characterized by elemental analyses, IR spectroscopy and single-crystal X-ray diffraction. Interestingly, compound 3 has been previously described in the literature [9]. Thus, the authors have also assayed this reaction with acetonitrile as solvent.

The elemental analyses for compounds 1–3 agree with the proposed formula. The IR spectra of 1–3 display the characteristic carboxylate bands in the range 1621–1615 cm 1 for mas(CO2) and 1429–1423 cm 1 for ms(CO2) (Supporting Information Figs. S1, S2 and S3, respectively). The difference between mas(CO2) and ms(CO2), for three compounds, is 192 cm 1, indicating bidentate bridging coordination mode of the acetate group [10,11]. The bands attributable to the aromatic groups m(C@C)ar, m(C@N)ar, d(CAH)ip and d (CAH)oop are also observed [12]. The IR spectral data thus clearly lend support to the structures determined by the X-ray diffraction method. UV–Vis electronic spectra of the synthesised complexes were measured in methanol solution. All spectra show one band in the visible region, between 706 and 682 nm with e = 36–11 mol 1 cm 1 l (Supporting Information Figs. S4, S5 and S6, respectively). These values are characteristic of Cu(II) complexes [13].

2.2. Crystal structure of complexes 1–3

The reaction of [Cu(m-MeCO2)2(H2O)]2 and 3-phenylpyridine (3-Phpy) (1), 2-benzylpyridine (2-Bzpy) (2) and 4-acetylpyridine (3), in methanol at room temperature with ratio 1:1, leads [Cu (MeCO2)2(3-Phpy)]2 (1), [Cu(MeCO2)2(2-Bzpy)]2 (2) and [Cu (MeCO2)2(4-Acpy)]2 (3) compounds. Perspective views of 1–3 are shown in Figs. 1–3 and selected distances and angles are provided in Tables 1–3, respectively.

The crystal structure of 1–3 confirmed that the three compounds have a paddle-wheel binuclear Cu(II) structures, with four bridging acetate ligands in a syn–syn coordination mode. The Cu Cu separation in 1–3 compounds are 2.6276(3), 2.6635(18) and 2.6317(3) Å, respectively, with values comparable to those reported for paddle-wheel complexes with similar structure [7,8,14–16]. The tetra-carboxylate bridging framework accommodates a metal–metal separation up to 3.452 Å [17].

Each Cu metal atom was coordinated to four oxygen atoms from two acetate groups at the equatorial positions and one nitrogen atom from amine derivatives at the apical position completing the slightly distorted square pyramidal coordination geometry (s = 0.0077 (1), 0.012 (2) and 0.0083 (3) [18]. The CuAO bond distances [CuAO: 1.9693–1.9733 Å (1); 1.959–1.983 Å (2) and 1.9653–1.9693 Å (3)] are

slightly shorter than CuAN bond distances [CuAN: 2.1633 Å (1); 2.245 Å (2) and 2.1928 Å (3)] due to the Jahn–Teller effect. The values are comparable with the reported values in [Cu2(m-MeCO2)2(L)]2 (L = 4-dimethylaminopyridine [19], nicotinamide [20], N-2-acetamidopyridine [21], 2-[N-(2-pyridyl)-carbamoyl]pyridine18 and 4-pyridylmethanol [22].

2.3. Extended structures of 1–3

The main difference between the three compounds is the intermolecular hydrogen bonding interactions. In all complexes, noncovalent CAH⋯O are observed while CAH⋯N is only observed in 1 (Table 4). In compound 1, four different CAH⋯O intermolecular hydrogen bonding interactions are observed. In these interactions, the oxygen atoms of the carboxylate groups are linked to CAH corresponding mainly to phenyl and pyridine ring of the ligand (3- Phpy). Additionally, one weak CAH⋯N intermolecular interaction is found (3.4731 Å; 138°). Due to these interactions, the extended supramolecular crystal structure can be described as 2-D compact arrangement (Fig. 4) [23]. In compound 2, the two most important intermolecular hydrogen bonding interactions involve CAH hydrogens of the phenyl ring and two non-equivalent oxygens of the acetates, leading also to the formation of a truly 2D supramolecular network (Fig. 5). In compound3, the oxygen atom of the 4-acetylpyridine ligand is linked to CAH hydrogen of the pyridine ring of an adjacent ligand, forming a 2-D layer (C6AO1⋯H4; Table 4). Additionally, intermolecular hydrogen bonding interactions between antiparallel acetate groups (C11AH11B⋯O5; Table 4), link adjacent bi-dimensional layers yielding to the formation of a three-dimensional supramolecular network (Fig. 6). Regarding intramolecular interactions, they are present in 1–3 complexes (Supporting Information Table S1) involving acetate groups. Nevertheless, all of them can be considered ‘‘weak” considering their angles (<120°).

3. CONCLUSIONS

In this paper, we described three acetate complexes (1–3) formed by [Cu(m-MeCO2)2]2 paddle-wheel units and different pyridine ligands (3-phenylpyridine (1), 2-benzylpyridine (2) and 4- acetylpyridine (3)) coordinated to the apical positions of copper. These compounds have been fully characterized to investigate their preparation and structural properties. The crystal structure confirmed that all of them have a paddle-wheel binuclear Cu(II) structure, with 4 bridging acetate ligands in a syn–syn coordination mode disposition. Finally, we have studied the extended structure of the Cu(II) complexes through weak intra- and intermolecular interactions in the outer sphere of the metal sites yielding bidimensional (1 and 2) or three-dimensional (3) supramolecular final arrangement. In all complexes, non-covalent CAH□ □ □ O are observed while CAH□ □ □ N is only observed in 1.

4. EXPERIMENTAL

4.1. Materials and general details

Cu(II) acetate monohydrate (Cu(MeCO2)2 H2O), 3-phenylpyridine (3-Phpy), 2-benzylpyridine (2-Bzpy) and 4-acetylpyridine (4-Acpy) ligands and methanol (MeOH) as a solvent, were purchased from Sigma–Aldrich and used without further purification. All reactions and manipulation were carried out in air. Elemental analyses (C, H, N) were carried out by the staff of Chemical Analysis Service of the Universitat Autònoma de Barcelona on a Thermo Scientific Flash 2000 CHNS Analyses. In the CHNS analyses, accomplished by combustion analysis, 0.7 mg of each sample was burned (1200 C) in an excess of oxygen and various traps, collecting the combustion products: CO2, H2O, N2 and SO2. Finally, they were analyzed and quantified by gas chromatography.

IR spectra were recorded at the Chemical Analysis Service of the Universitat Autònoma de Barcelona on a Tensor 27 (Bruker) spectrometer, equipped with an attenuated total reflectance (ATR) accessory model MKII Golden Gate with diamond window in the range 4000–600 cm 1. Electronic spectra in solution were run Kontron- Uvikon 860 in methanol, between 800 and 350 nm

4.2. Synthesis of the compounds [Cu(MeCO2)2(3-Phpy)]2 (1), [Cu (MeCO2)2(2-Bzpy)]2 (2) and [Cu(MeCO2)2(4-Acpy)]2 (3)

To a solution of (0.608 mmol) 3-phenylpyridine (3-Phpy) (94.3 mg), 2-benzylpyridine (103 mg) or 4-acetylpyridine (73.6 mg) in methanol 20 ml, Cu(MeCO2)2 H2O (0.545 mmol, 109 mg) in methanol (25 ml) was added. The two solutions turned turquoise and then were concentred almost to dryness. The green crystalline solids are formed. The compounds were filtered, washed with cold methanol and dried under vacuum.

1. Yield: 147 mg (82.0%). Anal. Calc. for C30H30N2O8Cu2: C, 53.59; H, 4.49; N, 4.16. Found: C, 53.32; H, 4.37; N, 4.01%. IR (KBr, cm 1) m: 1615(s) [mas(COO)], 1596(m) [m(C@C), m(C@N)], 1472(w) [m(C@C), m(C@N)], 1423(s) [ms(COO)], 1344(w), 1191(w), 1110(w), 1031(w), 823(w), 765(s), 707(s), 677(s) [d(CAH)oop], 624(m). UV–Vis (CH3OH, 9.96 10 3 M), k(e) = 699 (36) nm.

2. Yield: 143 mg (74.8%). Anal. Calc. for C32H34N2O8Cu2: C, 54.77; H, 4.88; N, 3.99. Found: C, 54.62; H, 4.85; N, 3.75%. IR (KBr, cm 1) m: 1616(s) [mas(COO)], 1602(m) [m(C@C), m(C@N)], 1581(w), 1484(w) [m(C@C), m(C@N)], 1454(w), 1424(s) [ms(COO)], 1345(m), 1058(w), 1012(w), 765(m), 747(m), 724(w), 703(w), 676(s) [d(CAH)oop], 622(s). UV–Vis (CH3OH, 5.90 10 2 M), k(e) = 682 (12) nm.

3. Yield: 112 mg (68.0%). Anal. Calc. for C22H26N2O10Cu2: C, 43.64; H, 4.63; N, 4.33. Found: C, 43.35; H, 4.57; N, 4.25%. IR (KBr, cm 1) m: 1696(m) [mas(CO)]acetyl, 1621(s) [mas(COO)], 1555(w) [m (C@C), m(C@N)], 1429(s) [ms(COO)], 1413(s), 1365(m), 1318(w), 1259(s), 1225(w), 1060(w), 1012(w), 833(m), 683(s) [d(CAH)oop], 631(m). UV–Vis (CH3OH, 6.51 10 3 M), k(e) = 706 (11) nm.

4.3. X-ray crystallography

For compound 1–3, a green prism-like specimen was used for the X-ray crystallographic analysis. The X-ray intensity data were measured on a D8 Venture system equipped with a multilayer mono-chromate and a Mo microfocus (k = 0.71073 Å). For 1–3, the frames were integrated with the Bruker SAINT Software package using a narrow-frame algorithm. For 1, the integration of the data using a monoclinic unit cell yielded a total of 115,095 reflections to a maxim h angle of 30.57° (0.70 Å resolution), of which 8857 were independent (average redundancy 12.995, completeness = 99.8%), Rint = 6.37%, Rsig = 3.02%) and 7016 (79.21%) were greater than 2r(F2). The calculated minimum and maximum transmission coefficients (based on crystal size) are 0.6347 and 0.7461. For 2, the integration of the data using a monoclinic unit cell yielded a total of 19,058 reflections to a maxim h angle of 26.62° (0.79 Å resolution), of which 3185 were independent (average redundancy 5.984, completeness = 98.5%), Rint = 9.71%, Rsig = 6.01%) and 2106 (66.12%) were greater than 2r(F2). The calculated minimum and maximum transmission coefficients (based on crystal size) are 0.6173 and 0.7454. For 3, the integration of the data using a monoclinic unit cell yielded a total of 40,533 reflections to a maxim h angle of 30.57° (0.70 Å resolution), of which 3775 were independent (average redundancy 10.737, completeness = 99.6%), Rint = 3.17%, Rsig = 1.72%) and 3377 (89.46%) were greater than 2r (F2). The calculated minimum and maximum transmission coefficients (based on crystal size) are 0.6920 and 0.7461.

The structures were solved using the Bruker SHELXTL Software, package and refined using SHELX [24]. For 1, the final anisotropic full-matrix least-squares refinement on F2 with 383 variables converged at R1 = 3.38%, for the observed data and wR2 = 7.72% for all data. For 2, the final anisotropic full-matrix least-squares refinement on F2 with 200 variables converged at R1 = 8.44%, for the observed data and wR2 = 17.36% for all data. For 3, the final anisotropic full-matrix least-squares refinement on F2 with 165 variables converged at R1 = 2.48%, for the observed data and wR2 = 5.91% for all data. For 1–3, the final cell constants and volume, are based upon the refinement of the XYZ-centroids of reflections above 20 r(I). Data were corrected for absorption effects using the multi-scan method (SADABS). Crystal data and relevant details of structure refinement for compounds 1–3, are reported in Table 5. Complete information about the crystal structure and molecular geometry is available in CIF format as Supporting Information. CCDC 1545879 (1), 1545880 (2), and 1545881 (3) contain the supplementary data for this paper as well as the IR and UV–Vis spectra. Molecular graphics were generated with the program Mercury 3.6 [25,26]. Color codes for all molecular graphics: blue (Cu), light blue (N), red (O), grey (C), white (H).

ACKNOWLEDGEMENTS

This work was financed by the Spanish National Plan of Research MAT2015-65756-R and by 2014SGR260 and 2014SGR377 projects from the Generalitat de Catalunya – Spain.

REFERENCES

[1] (a) E. Coronado, J.R. Galan-Mascaros, P. Gaviña, C. Martí-Gastaldo, F.M. Romero, S. Tatay, Inorg. Chem. 47 (2008) 5197; (b) X.-Y. Li, L.-Q. Liu, M.-L. Ma, X.-L. Zhao, K. Wen, Dalton Trans. 39 (2010) 8646.

[2] L. Cui, Y.-F. Geng, C.F. Leong, Q. Ma, D.M. D'Alessandro, K. Deng, Q.-D. Zeng, J.-L. Zuo, Sci. Rep. 6 (2016) 1.

[3] For examples, see: (a) C.-S. Liu, J.-J. Wang, L.-F. Yan, Z. Chang, X.-H. Bu, E.C. Señudo, J. Ribas Inorg. Chem. 46 (2007) 6299; (b) B. Moulton, M.J. Zaworotko, Chem. Rev. 101 (2001) 1629; (c) A.J. Blake, N.R. Champness, P. Hubberstey, W.-S. Li, M.A. Withersby, M. Schröder, Coord. Chem. Rev. 183 (1999) 117; (d) M. Kato, Y. Muto, Coord. Chem. Rev. 92 (1988) 45.

[4] (a) J. Moncol, M. Mudra, P. Lónnecke, M. Hewitt, M. Valko, H. Morris, J. Svorec, M. Melnik, M. Mazur, M. Koman, Inorg. Chim. Acta 360 (2007) 3213; (b) G.C. Campbell, J.F. Haw, Inorg. Chem. 27 (1988) 3706.

[5] For examples, see: (a) N. Abdullah, Y. Al-Hakem, N. Abdullah, H. Samsudin, N.S. A. Tajidi, Asian J. Chem. 26 (2014) 987; (b) R. Sarma, J.B. Baruah, J. Coord. Chem. 61 (2008) 3329; (c) R. Cejuto, G. Alzuet, J. Borrás, M. Liu-Gonzalez, F. Sanz-Ruiz, Polyhedron 21 (2002) 1057; F.P.W. Agterberg, H.A.J. Provó Kluit, W.L. Driessen, H. Oevering, W. Buijs, M.T. Lakin, A.L. Spek, J. Reedjick, Inorg. Chem. 36 (1997) 4321.

[6] M. Guerrero, S. Vázquez, J.A. Ayllón, T. Calvet, M. Font-Bardía, J. Pons, ChemistrySelect 2 (2017) 632.

[7] J. Soldevila-Sanmartín, J.A. Ayllón, T. Calvet, M. Font-Bardía, J. Pons, Polyhedron 126 (2017) 184.

[8] J. Soldevila-Sanmartín, J.A. Ayllón, T. Calvet, M. Font-Bardía, C. Domingo, J. Pons, Inorg. Chem. Commun. 71 (2016) 90.

[9] S. Youngme, A. Cheansirisomboon, C. Danvirutai, C. Pakawatchai, N. Chaichit, C. Engkagul, G.A. van Albada, J. Sánchez-Costa, J. Reedijk, Polyhedron 27 (2008) 1875.

[10] K. Nakamoto, Infrared and Raman spectra of inorganic and coordination compounds, in: Applications in Coordination, Organometallic and Bioinorganic Chemistry, sixth ed., Wiley Interscience, New York, USA, 2009.

[11] G.B. Deacon, R.J. Phillips, Coord. Chem. Rev. 88 (1980) 227.

[12] D.H. Williams, I. Fleming, Spectroscopic Methods in Organic Chemistry, McGrawHill, London, UK, 1995.

[13] (a) D. Sutton, Electronic Spectra of Transition Metal Complexes, McGraw-Hill, London, UK, 1975; (b) M. Guerrero, T. Calvet, M. Font-Bardía, J. Pons, Polyhedron 119 (2016) 555.

[14] R.C. Santra, K. Sengupta, R. Dey, T. Shireen, P. Das, P.S. Guin, K. Mulkhopadhyay, S. Das, J. Coord. Chem 67 (2014) 265.

[15] M. Barquín, N. Cocora, M.J.G. Garmendia, L. Larrínaga, E. Pinilla, M.R. Torres, J. Coord. Chem. 63 (2010) 2247.
[16] A.V. Yakovenko, S.V. Kolotilov, O. Cador, S. Golhen, L. Ouahab, V.V. Pavlishchuck, Eur. J. Inor. Chem. (2009) 2354.
[17] T. Allman, R.C. Goel, N.K. Jha, A.L. Beauchamp, Inorg. Chem. 23 (1984) 914.
[18] W. Addison, T.N. Rao, J. Chem. Soc., Dalton Trans. (1984) 1349.
[19] X.-Jun Feng, H.-Ze Dong, W. Huang, Acta Cryst. E63 (2007) m1105.
[20] B. Kozlevcar, I. Leban, I. Turel, P. Segedin, M. Petric, F. Pohleven, A.J.P. White, D. J. Williams, J. Sieler, Polyhedron 18 (1999) 755.
[21] M.A. Pauly, E.M. Erwin, D.R. Powell, G.T. Rowe, L. Yang, Polyhedron 102 (2015) 722.
[22] N.N. Hoang, F. Valach, M. Melnik, Acta Cryst. C49 (1993) 467.
[23] Th. Steiner, Cryst. Rev. 6 (1996) 1.
[24] G.M. Sheldrick, Acta Cryst. C71 (2015) 3.
[25] C.F. Macrae, P.R. Edgington, P. McCabe, E. Pidcock, G. Shields, R. Taylor, M. Towler, J. van de Streek, J. Appl. Crystallogr. 39 (2006) 453.
[26] C.F. Macrae, I.J. Bruno, J.A. Chisholm, P.R. Edgington, P. McCabe, E. Pidcock, I. Rodriguez-Monge, R. Taylor, J. van de Streek, P.A. Wood, J. Appl. Crystallogr. 41 (2008) 466.

Legends to figures

Figure. 1 ORTEP diagram of the [Cu(MeCO2)2(3-Phpy)]2 (1) complex showing an atom labelling scheme. 50% probability of the amplitude displacement ellipsoids is shown. The hydrogen atoms are omitted for clarity. See Table 1 for selected values of bond lengths and bond angles.

Figure. 2 ORTEP diagram of the [Cu(MeCO2)2(2-Bzpy)]2 (2) complex showing an atom labelling scheme. 50% probability of the amplitude displacement ellipsoids is shown. The hydrogen atoms are omitted for clarity. See Table 2 for selected values of bond lengths and bond angles.

Figure. 3 ORTEP diagram of the [Cu(MeCO2)2(4-Acpy)]2 (3) complex showing an atom labelling scheme. 50% probability of the amplitude displacement ellipsoids is shown. The hydrogen atoms are omitted for clarity. See Table 3 for selected values of bond lengths and bond angles.

Figure. 4 Three-dimensional ordering of the [Cu(MeCO2)2(3-Phpy)]2 (1) units generated by intermolecular CAH□ □ □ O and CAH□ □ □ N hydrogen bonding interactions. (left (100) direction; right (001) direction).

Figure. 5 Three-dimensional ordering of the [Cu(MeCO2)2(2-Bzpy)]2 (2) units generated by intermolecular CAH□ □ □ O hydrogen bonding interactions. (left (010) direction; right (001) direction).

Figure. 6 Three-dimensional ordering of the [Cu(MeCO2)2(4-Acpy)]2 (3) units generated by intermolecular CAH□ □ □ O and CAO□ □ □ H hydrogen bonding interactions. (top (010) direction; bottom (001) direction)..

FIGURE 1

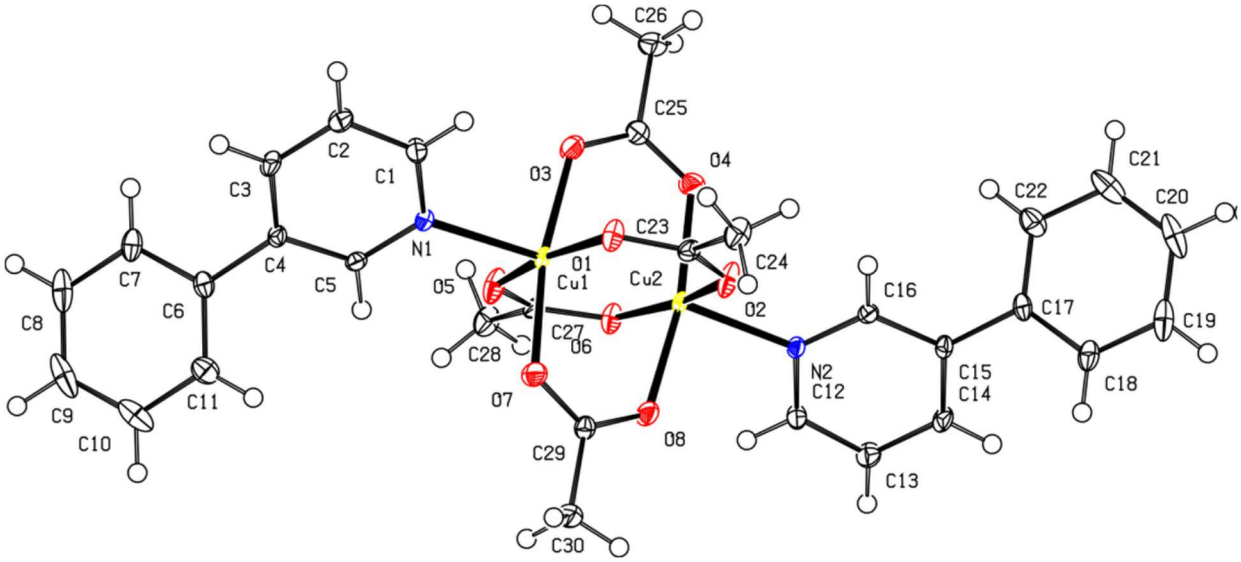
C26
C25
C2
C1
O3
O4
C21
C3
C22
C20
C23
N1
O1
C24
C7
C4
C5
O5
Cu1
Cu2
C16
C8
C6
C27
O2
C17
C19
C28
O6
N2
C15
C18
O7
C12
C14
C9
C11
O8
C29
C13
C10
C30

FIGURE 2

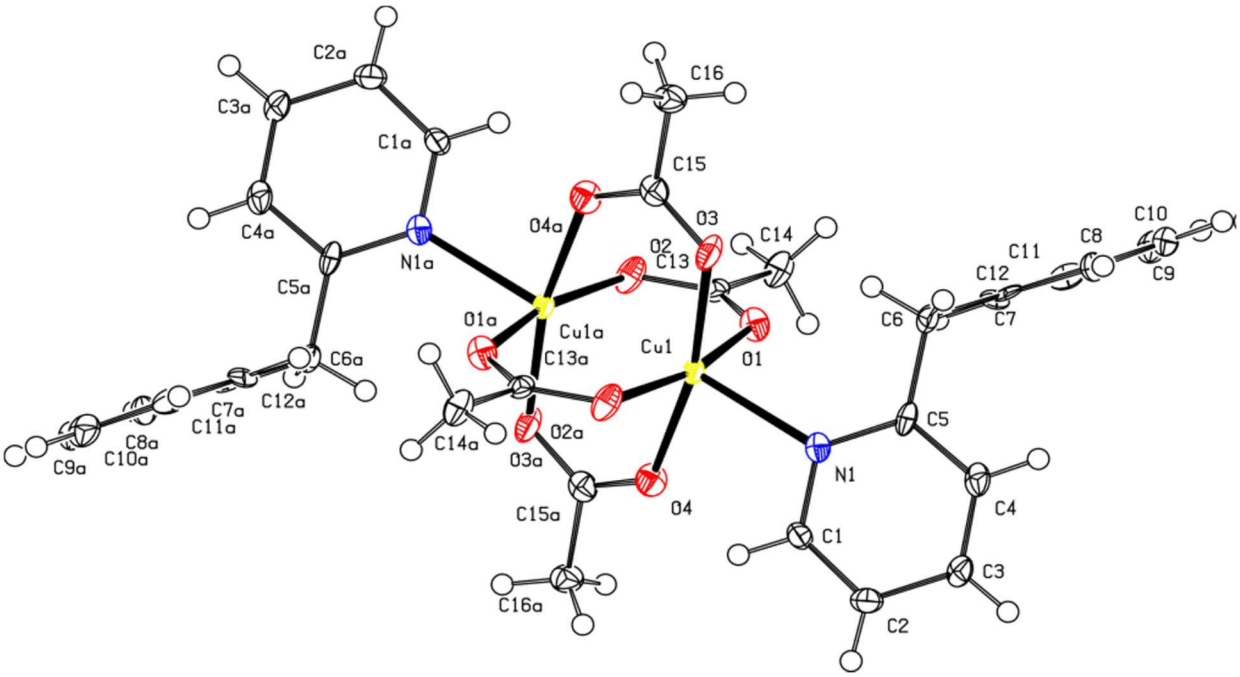
C2a
C3a
C1a
C16
C15
C4a
N1a
O4a
O3
O2
C13
C14
C10
C11
C8
C12
C9
C5a
O1a
Cu1a
Cu1
O1
C6
C7
C6a
C13a
C7a
C12a
C11a
C8a
C10a
C9a
C14a
O2a
O3a
C5
N1
C4
O4
C15a
C1
C3
C16a
C2

316 **FIGURE 3**

317

318

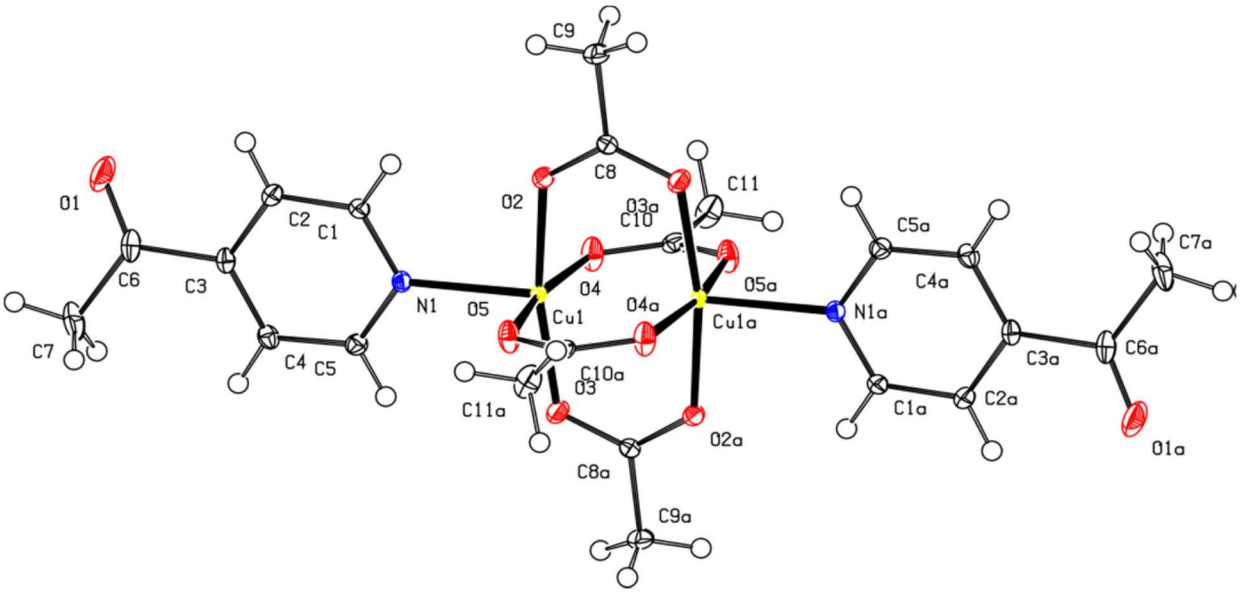

319

320

FIGURE 4

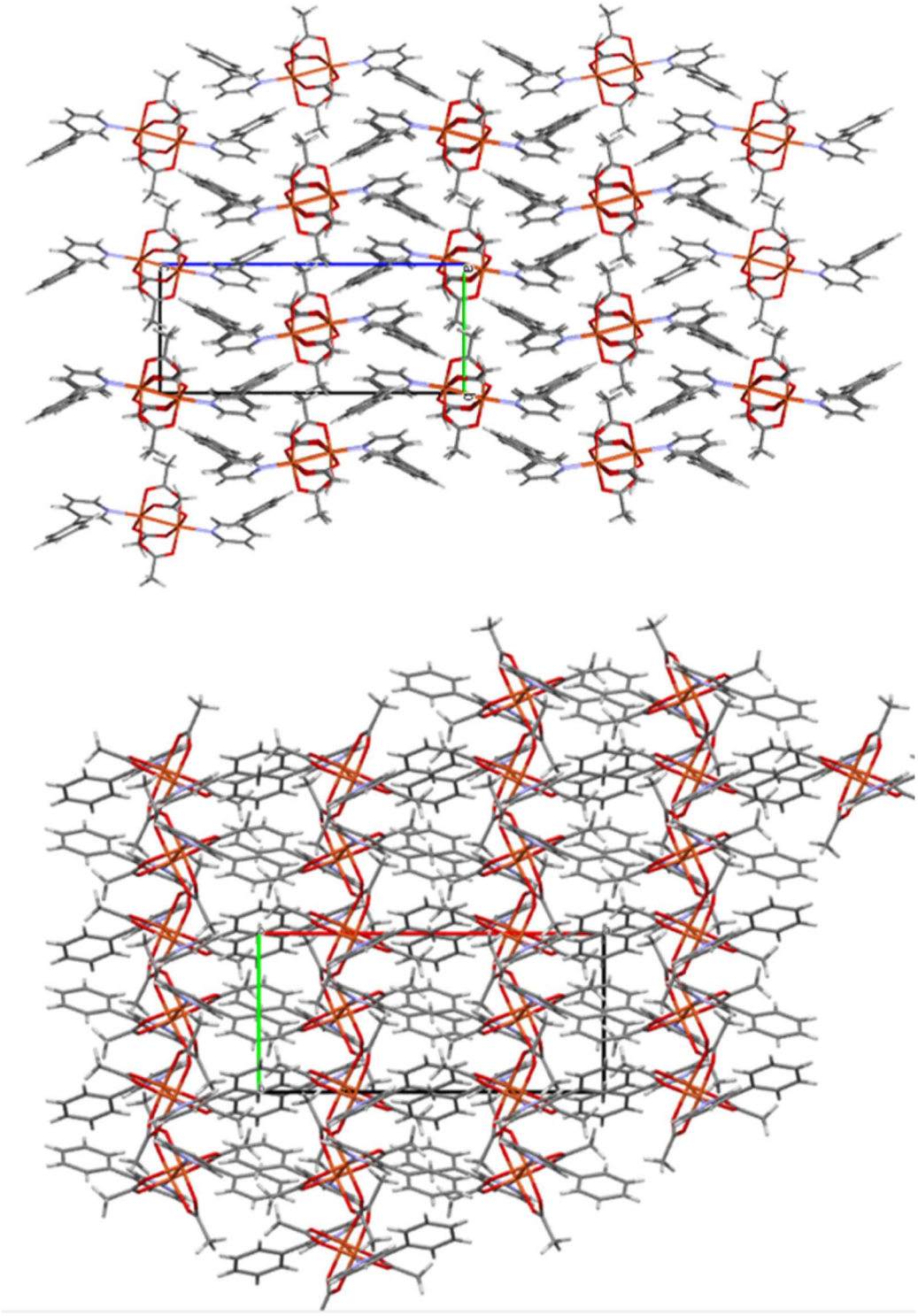

FIGURE 5

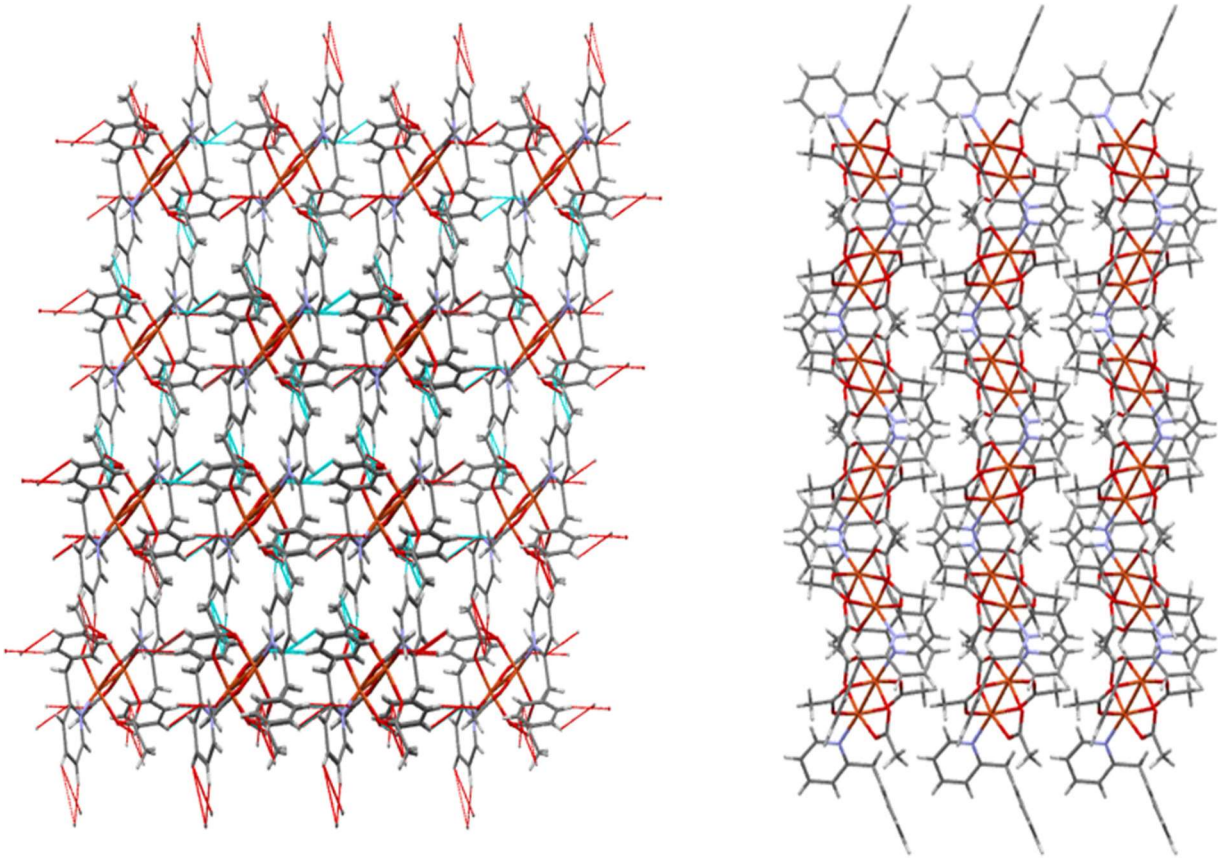

336 **FIGURE 6**

337

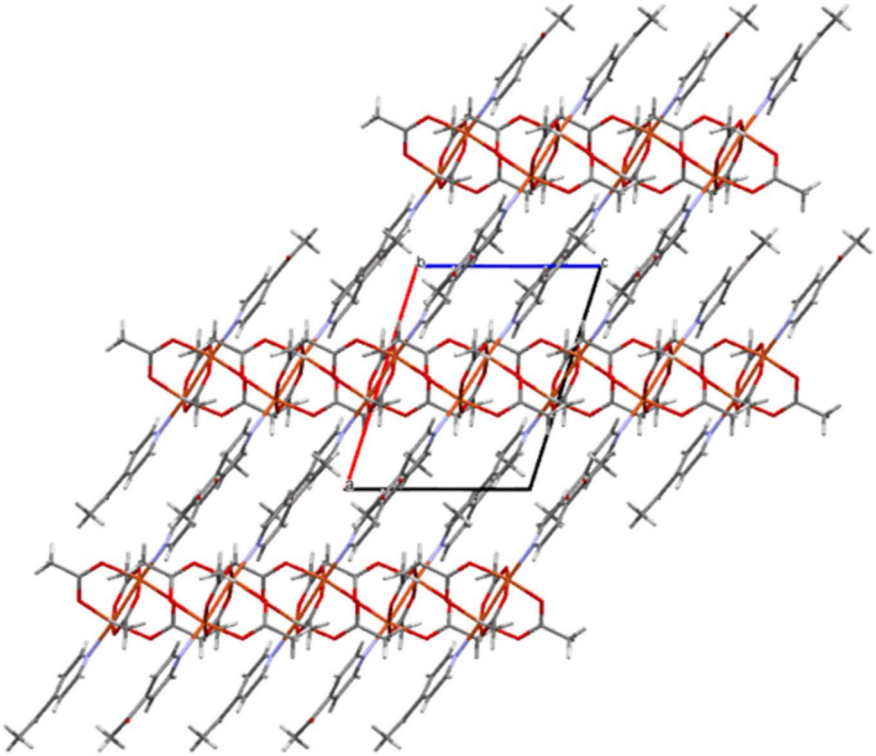

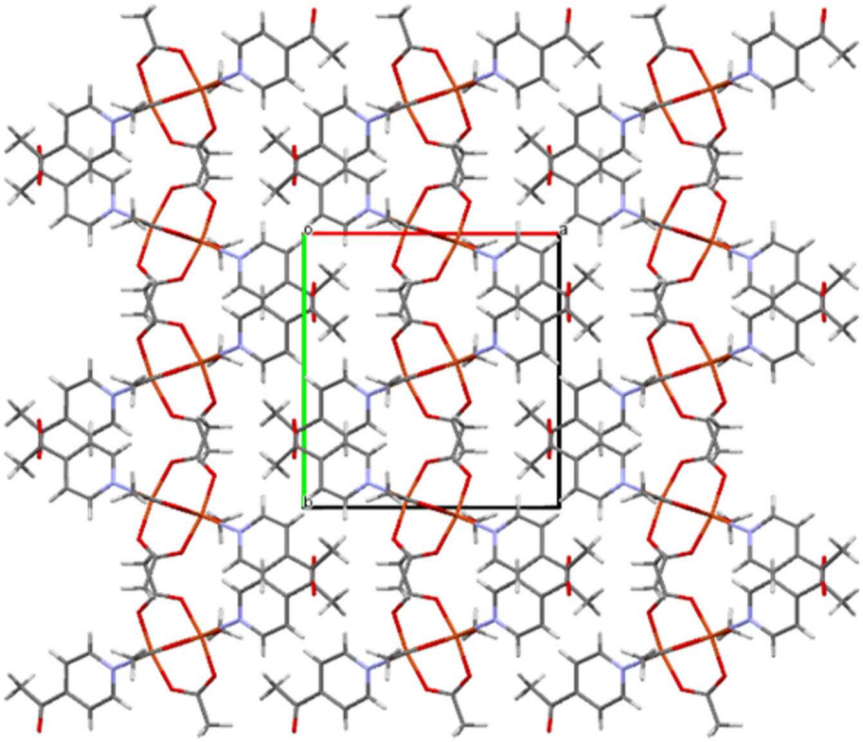

338

339

Table 1 Selected bond lengths (Å) and bond angles (°) for 1.

Bond length (Å)			
Cu(1)—O(5)	1.9693(12)	Cu(1)—O(3)	1.9711(12)
Cu(1)—O(1)	1.9706(12)	Cu(1)—O(7)	1.9733(12)
Cu(1)—N(00B)	2.1653(13)	Cu(1)—Cu(2)	2.6276(3)
Bond angles (°)			
O(5)—Cu(1)—O(1)	168.11(5)	O(5)—Cu(1)—O(7)	89.04(6)
O(5)—Cu(1)—O(3)	89.75(6)	O(1)—Cu(1)—O(7)	90.23(6)
O(1)—Cu(1)—O(3)	88.62(6)	O(3)—Cu(1)—O(7)	168.57(5)
O(5)—Cu(1)—N(00B)	91.75(5)	O(3)—Cu(1)—N(00B)	95.03(5)
O(1)—Cu(1)—N(00B)	100.13(5)	O(7)—Cu(1)—N(00B)	96.37(5)

346 **Table 2** Selected bond lengths (Å) and bond angles ( ) for 2.

347

Bond length (Å)			
Cu(1)—O(1)	1.959(5)	Cu(1)—O(2)#1	1.971(5)
Cu(1)—O(3)	1.964(5)	Cu(1)—O(4)	1.983(5)
Cu(1)—N(1)	2.245(6)	Cu(1)—Cu(1)#1	2.6635(18)
Bond angles (°)			
O(1)—Cu(1)—O(3)	88.6(2)	O(1)—Cu(1)—O(2)#1	166.5(2)
O(1)—Cu(1)—O(4)	91.4(2)	O(3)—Cu(1)—O(2)#1	88.3(2)
O(3)—Cu(1)—O(4)	167.2(2)	O(2)#1—Cu(1)—O(4)	88.7(2)
O(1)—Cu(1)—N(1)	96.3(2)	O(2)#1—Cu(1)—N(1)	97.2(2)
O(3)—Cu(1)—N(1)	102.7(2)	O(4)—Cu(1)—N(1)	90.0(2)

348

349

350

Table 3 Selected bond lengths (Å) and bond angles (°) for 3.

Bond length (Å)			
Cu(1)—O(5)#1	1.9653(10)	Cu(1)—O(3)#1	1.9658(10)
Cu(1)—O(4)	1.9676(10)	Cu(1)—O(2)	1.9693(10)
Cu(1)—N(1)	2.1928(11)	Cu(1)—Cu(1)#1	2.6317(3)
Bond angles (°)			
O(5)#1—Cu(1)—O(3)#1	89.45(5)	O(5)#1—Cu(1)—O(4)	168.42(4)
O(3)#1—Cu(1)—O(4)	88.95(5)	O(5)#1—Cu(1)—O(2)	89.50(5)
O(3)#1—Cu(1)—O(2)	168.47(4)	O(4)—Cu(1)—O(2)	89.78(5)
O(5)#1—Cu(1)—N(1)	94.23(4)	O(3)#1—Cu(1)—N(1)	98.23(4)
O(4)—Cu(1)—N(1)	97.35(4)	O(2)—Cu(1)—N(1)	91.31(4)

Table 4 Distances [Å] and angles [□] related to hydrogen bonding interactions in complexes 1–3**.**

1	[Å]	[Å]	[°]	
D—H···A	H···A	D···A	>D—H···A	Symmetry
C2-H2···O5	2.566	3.312	135.64	3/2 − x, ½ + y, 3/2 − z
C7-H7···O1	2.526	3.442	162.01	x, y, z
C18-H18···O6[i]	2.540	3.460	163.37	x, 1 + y, 1 + z
C24-H24C···O6[ii]	2.582	3.428	144.65	3/2 − x, ½ + y, 3/2 − z
C9-H9···N00C	2.708	3.473	138.00	−½ + x, ½ − y, ½ + z
2				
C10-H10A···O4	2.620	3.414	143.74	x, −1 + y, z
C8-H8A···O2	2.707	3.626	169.12	x, ½ − y, ½ + z
3				
C11-H11B···O5	2.586	3.520	159.36	1 − x, 1 − y, 1 − z
C6-O1···H4	2.711	3.901	167.08	1 − x, 1 − y, −z

363 **Table 5** Crystallographic data for 1–3.

364

	1	2	3
Empirical formula	$C_{30}H_{30}Cu_2N_2O_8$	$C_{28}H_{34}Cu_2N_2O_8$	$C_{22}H_{20}Cu_3N_2O_{10}$
Formula weigh	673.64	701.69	605.53
T (K)	100(2)	293(2)	100(2)
λ (Å)	0.71073	0.71073	0.71073
System, space group	monoclinic, $P2_1/n$	monoclinic, $P2_1/c$	monoclinic, $P2_1/c$
Unit cell dimensions			
a (Å)	18.0025(10)	7.8581(8)	11.5737(6)
b (Å)	8.2631(4)	11.2348(13)	12.9188(6)
c (Å)	19.4947(11)	17.6990(19)	8.6005(4)
α (°)	90	90	90
β (°)	93.563(2)	98.435(7)	106.70(2)
γ (°)	90	90	90
V (Å^3)	2894.4(3)	1545.6(3)	1231.69(10)
Z	4	2	2
D_{calc} (g cm^{-3})	1.546	1.508	1.633
μ (mm^{-1})	1.523	1.430	1.785
$F(000)$	1384	724	620
Crystal size (mm^3)	0.587 × 0.388 × 0.285	0.128 × 0.078 × 0.075	0.158 × 0.105 × 0.096
hkl ranges	$-25 \le h \le 25$ $-11 \le k \le 11$ $-25 \le l \le 27$	$-9 \le h \le 9$ $-14 \le k \le 14$ $-22 \le l \le 22$	$-16 \le h \le 15$ $-18 \le k \le 18$ $-10 \le l \le 12$
2θ range (°)	2.093–30.574	2.327–26.616	2.421–30.569
Reflections collected/unique/$\lvert R_{int}\rvert$	115095/8857/$\lvert R_{int}\rvert$ = 0.0637	19058/3185/$\lvert R_{int}\rvert$ = 0.0971	40533/3775/$\lvert R_{int}\rvert$ = 0.0317
Completeness to θ = 25.240	99.9%	99.8%	99.8
Absorption correction	semi-empirical	semi-empirical	semi-empirical
Max. and min. transmis.	0.7461 and 0.6347	0.7454 and 0.6173	0.7461 and 0.6920
Refinement method	full matrix least-squares on F^2	full matrix least-squares on F^2	full matrix least-squares on F^2
Data/restrains/parameters	8857/0/383	3185/0/200	3775/0/165
Goodness-of-fit (GOF) on F^2	1.040	1.175	1.065
Final R indices [$I > 2\sigma(I)$]	R_1 = 0.0838, wR_2 = 0.0710	R_1 = 0.0844, wR_2 = 0.1581	R_1 = 0.0248, wR_2 = 0.0572
R indices (all data)	R_1 = 0.0529 wR_2wR_2 = 0.0772	R_1 = 0.1398 wR_2 = 0.1736	R_1 = 0.0308 wR_2 = 0.0591
Extinction coefficient	n/a	n/a	n/a
Largest. Diff. peak and hole (e Å^{-3})	0.479 and −0.460	0.909 and −0.826	0.472 and −0.421

365